ANIMAL STUDY

e-ISSN 1643-3750
© Med Sci Monit, 2026; 32: e954263
DOI: 10.12659/MSM.954263

Received: 2026.05.28
Accepted: 2026.06.01
Available online: 2026.06.15
Published: 2026.XX.XX

Isopsoralen Promotes Mandibular Fracture Healing by Regulating Autophagy

Authors' Contribution:
Study Design A
Data Collection B
Statistical Analysis C
Data Interpretation D
Manuscript Preparation E
Literature Search F
Funds Collection G

ABCDEF 1 Bing Xu
ABCD 1 Ruoyu Mei
BCD 1 Shizhu Du
BCD 1 Zhijiang Zou
BCD 1 Kehan Chen
BCD 1 Guoao Zhou
AG 1 Fang Wang
AFG 1,2 Wei He

1 School and Hospital of Stomatology, Zunyi Medical University, Zunyi, Guizhou, PR China
2 The Fifth Affiliated Hospital of Zunyi Medical University, Zhuhai, Guangdong, PR China

Corresponding Authors: Fang Wang, School and Hospital of Stomatology, Zunyi Medical University, No. 143, Dalian Road, Huichuan District, Zunyi, Guizhou 563000, China, e-mail: 214185396@qq.com; Wei He, The Fifth Affiliated Hospital of Zunyi Medical University, zhufengdadao No.1439, Doumen District, Zhuhai, Guangdong 519100, China, e-mail: heweichenhui@126.com

Financial support: This study was supported by the "12345 Future Leading Clinicians" Talent Development Program of Zunyi Medical University (20221004; project director: Fang Wang) and the Zunyi Scientific and Technological Innovation Team Construction Project (grant No. ZunKCTD051)

Conflict of interest: None declared

Background: Mandibular fractures account for 40% to 65% of maxillofacial injuries, with about 10% developing delayed union or nonunion. Isopsoralen (ISO), a main active component of *Psoralea corylifolia* L., exhibits osteogenic and anti-inflammatory effects. However, the role of autophagy in ISO-promoted mandibular fracture healing remains unclear. This study aimed to investigate the effects of ISO on mandibular fracture healing in rats and its underlying autophagy-mediated mechanism.

Material/Methods: Specific pathogen-free–grade rats with left mandibular fractures were randomly assigned to 4 groups: normal saline (NS), ISO, 3-methyladenine (3-MA), and ISO + 3-MA. Interventions were given every 2 days. Fracture healing was assessed at 2, 4, and 6 weeks using the Lane-Sandhu radiographic scoring system, micro-computed tomography, hematoxylin-eosin staining, enzyme-linked immunosorbent assay, and western blotting.

Results: Compared with other groups, the 3-MA group showed impaired healing, with lower radiographic scores, bone volume/total volume, bone mineral density, and trabecular number; higher trabecular separation; and sparse bone formation (all $P < 0.05$). Relative to the NS group, the ISO group exhibited improved bone microarchitecture, elevated serum alkaline phosphatase and osteocalcin levels, and distinct autophagy marker changes (at 2 weeks: upregulated sequestosome 1 (P62), downregulated microtubule-associated protein 1 light chain 3 II/I (LC3-II/I); at 6 weeks: downregulated P62, Beclin-1, and LC3II/I; all $P < 0.05$). Autophagy indices in the ISO + 3-MA group were comparable to those in the ISO group ($P > 0.05$).

Conclusions: ISO stabilized autophagic flux and alleviated 3-MA-induced delayed mandibular fracture healing by regulating autophagy.

Keywords: mandibular fracture • autophagy • fracture healing

Full-text PDF: https://www.medscimonit.com/abstract/index/idArt/954263

Indexed in: [Current Contents/Clinical Medicine] [SCI Expanded] [ISI Alerting System] [ISI Journals Master List] [Index Medicus/MEDLINE] [EMBASE/Excerpta Medica] [Chemical Abstracts/CAS]

Introduction

Millions of fractures occur annually worldwide, representing a significant public health challenge. Fracture healing can be delayed by nonunion, a major cause of long-term patient disability [1]. Among the new fracture cases reported globally in 2019, facial fractures involving the craniofacial bones, jawbones, and related structures accounted for approximately one-third, affecting an estimated 1.5 million individuals [2]. Mandibular fractures are among the most common maxillofacial injuries, accounting for 40% to 65% of all facial fractures [3]. The etiology of maxillofacial fractures is multifactorial and includes traffic accidents, falls, sports-related injuries, and acts of violence [4,5]. Fracture healing is a multifaceted biological process that encompasses hematoma formation, callus formation, and bone remodeling [6]. Osteoblasts play crucial roles in bone tissue growth and the wound healing process. Impairments in osteoblast function can result in delayed fracture healing and worsen pathological changes in bone tissue [7]. Nonunion refers to a fracture that fails to heal within the expected period or is deemed incapable of healing without medical intervention. As a complex chronic condition, bone nonunion is often accompanied by persistent pain and can lead to functional impairment, long-term aesthetic concerns, and psychological distress [8]. Under the current standard of care for fractures, approximately 10% of patients experience delayed fracture union or nonunion. Therefore, medical interventions that can accelerate fracture repair hold significant clinical value, as they may facilitate the mitigation of fracture-related adverse outcomes, including delayed union and nonunion, thereby reducing the burden of associated complications.

Psoralea is a leguminous plant used in traditional Chinese medicine and is one of the primary components of the "Xianling Gubao capsule," a widely prescribed drug for preventing and treating osteoporosis [9]. *Psoralea corylifolia* L. is a natural estrogen modulator known for its diverse pharmacological effects, including enhancing cellular immune function, stimulating osteoblast activity, inhibiting osteoclasts, and exhibiting antibacterial and antiviral properties [10,11]. Isopsoralen (ISO), one of its main active ingredients, is known for its kidney-tonifying effects in traditional Chinese medicine [12]. ISO has multiple biological effects, including anti-inflammatory and osteogenic activities. Specifically, it can ameliorate bone metabolic disorders by regulating bone metabolism–related signaling pathways, promoting osteoblast differentiation, inhibiting osteoclast differentiation and proliferation, and alleviating inflammation and oxidative stress [13]. It is unknown whether ISO also possesses mechanisms to promote fracture healing in addition to these regulatory mechanisms.

Autophagy is a conserved catabolic pathway in eukaryotes, in which cytoplasmic components are encapsulated by a double membrane and degraded by lysosomes and vesicles, which plays a key role in maintaining cellular homeostasis and adapting to metabolic stress [14,15]. During fracture healing, autophagy participates in multiple critical processes, including early inflammatory regulation, osteoblast survival and differentiation, and bone matrix mineralization [16,17]. Abnormal autophagy function (either hyperactivation or inhibition) has been demonstrated to be closely associated with delayed fracture healing and nonunion [18,19]. Therefore, modulating autophagy activity has emerged as a potential strategy to promote fracture healing. Autophagy can be categorized into 3 forms—macroautophagy, microautophagy, and chaperone-mediated autophagy—on the basis of the morphological and functional distinctions in cytoplasmic cargo degradation. Among these, macroautophagy (hereafter referred to as autophagy) is the most extensively studied type [20]. Autophagy dysfunction is implicated in various human diseases, including cancer, metabolic disorders, immune diseases, and neurodegenerative conditions [21]. Importantly, autophagy is critically involved in bone metabolism and plays a vital role in maintaining the homeostasis of bone marrow-derived mesenchymal stem cells and their lineages, such as adipocytes, chondrocytes, and osteoblasts [17,22]. Autophagy, as a critical intracellular degradation system, plays a central role in early inflammatory initiation, bone remodeling, and bone metabolism during fracture healing. Its inhibition or overactivation can impair the healing process [23]. However, it remains unclear whether ISO facilitates fracture healing by modulating autophagy.

To investigate the role of autophagy in fracture healing, this study employed 3-methyladenine (3-MA) as a classical autophagy inhibitor. 3-MA inhibits autophagosome formation by blocking type III phosphatidylinositol 3-kinase, and has been widely applied in bone metabolism research [24]. By dynamically monitoring autophagy marker proteins Beclin-1 (autophagy initiation), microtubule-associated protein 1 light chain 3 II/I (LC3-II/I; autophagosome), and upregulated P62 (autophagy substrate degradation), the state of autophagy flow can be comprehensively evaluated [25,26]. In terms of osteogenic function, serum alkaline phosphatase (ALP), a zinc-containing glycoprotein expressed in various human tissues and organs, serves as a marker of early osteoblast differentiation and participates in matrix mineralization [27]. Osteocalcin (OCN) is a validated serum biomarker secreted by osteoblasts, used to reflect bone formation status [28]. ALP and OCN are classic indicators for evaluating osteogenic function in fracture healing studies.

This study established a model of autophagy inhibition in rat mandibular fracture and dynamically monitored the changes in the aforementioned autophagy and osteogenic markers. The aim was to investigate whether ISO promotes fracture healing by regulating cellular autophagy and preliminarily elucidate its

Indexed in: [Current Contents/Clinical Medicine] [SCI Expanded] [ISI Alerting System] [ISI Journals Master List] [Index Medicus/MEDLINE] [EMBASE/Excerpta Medica] [Chemical Abstracts/CAS]

mechanism of action, thereby providing experimental evidence for the precision treatment of mandibular fracture.

Material and Methods

Experimental Animals

A total of 80 healthy 9-week-old male Sprague-Dawley (SD) rats weighing 350 ± 10 g were used in this study. All rats, of specific pathogen-free grade, were obtained from the Experimental Animal Center of Zunyi Medical University (license number: SYXK (Qian) 2021-0004). The animals were housed in an specific pathogen-free facility at the same center under a standardized 12-hour light/dark cycle, with the room temperature maintained at 22 to 25 °C, and provided with ad libitum access to food and water. After 1 week of acclimation, the experiments were commenced. All experimental procedures were approved by the Animal Welfare and Ethics Committee of Zunyi Medical University (approval No. ZMU21-2411-078) and were conducted in strict accordance with the 3R principles (replacement, reduction, and refinement).

Drugs and Reagents

Sodium pentobarbital (batch No. 11715) was obtained from Sigma-Aldrich (St. Louis, MO, USA). ISO and 3-MA were obtained from Hubei Cuiyuan Biotechnology Co, Ltd (Wuhan, China). The following antibodies were used in this study: rabbit anti-Beclin 1 antibody and mouse anti-P62 antibody (cat. No. 11306-1-AP, 66184-1-Ig; Proteintech Group, Inc, Rosemont, IL, USA) and rabbit anti-LC3B antibody and goat anti-rabbit IgG H&L conjugated to horseradish peroxidase (HRP; cat. No. A7198, AS007; ABclonal Technology Co, Ltd, Wuhan, China). Additionally, an H&E staining kit was obtained from Wuhan Servicebio Technology Co, Ltd (Wuhan, China); a bicinchoninic acid protein quantification kit was obtained from Beijing Solebao Technology Co, Ltd (Beijing, China); and enzyme-linked immunosorbent assay (ELISA) kits for OCN and ALP were obtained from Shanghai Keaibo Biotechnology Co, Ltd (Shanghai, China).

Modeling and Experimental Grouping

An animal model was established by anesthetizing the rats with a 3% pentobarbital solution (40 mg/kg) and placing them in a supine position for skin disinfection. A bone incision, 1 mm in width and 3 mm in depth, was made via a slow micromotor and stainless steel grinding head at the intersection of the vertical projection line of the rat's mandibular third molar and the lower edge of the mandible, creating an incomplete mandibular fracture model. The surgical site was cleaned, sutured, and confirmed for successful modeling via radiography. Postoperatively, 80 ×10^5 U of penicillin was administered intramuscularly for 3 days to prevent infection.

After a 2-week postoperative observation period, 72 SD rats were randomly allocated to 4 groups using a random number table (n = 18 per group). Each group was further equally divided into 3 time-point subgroups for outcome evaluation at 2, 4, and 6 weeks after administration, with 6 rats per time point per group. The overall experimental design is shown in **Figure 1**. All interventions were administered once every 2 days via a dual-route strategy: oral gavage (2 mL) for ISO or sterile normal saline, and intraperitoneal injection (1 mL) for 3-MA or sterile normal saline (the detailed drug administration protocol is presented in **Table 1**). For all histological, serological, and molecular analyses, 3 independent biological samples were randomly selected from the 6 rats in each time-point subgroup for statistical testing.

Score of Fracture Healing Degree

At 2, 4, and 6 weeks following treatment, the left mandibles of the rats were harvested, and radiograph imaging was performed on the surgical-side mandibles to evaluate fracture line resolution and callus formation in each group. The Lane-Sandhu radiographic scoring system was used to evaluate the degree of bone reconstruction in the bone graft area, as shown in **Table 2** [29].

Micro-Computed Tomography Scan

Following drug intervention, the left mandibles of the rats were extracted at week 6 for ex vivo micro-computed tomography (micro-CT) scanning via an NMC-200 micro-CT scanner. The entire mandible was scanned, and subsequent 3-dimensional reconstruction was conducted via the Avatar image processing software. A region of interest measuring 1.5 mm along the left and right fracture lines was selected for analysis, with relevant parameters quantified and assessed via Cruiser software. The micro-CT scan focused on the mandibular fracture site, and CT Analyzer software was used to evaluate bone volume/total volume, bone mineral density, trabecular number, and trabecular separation.

H&E Staining

At 2, 4, and 6 weeks after administration, the left mandibles of the rats were removed, fixed in 4% paraformaldehyde for 2 days, decalcified, and paraffin-embedded. The thickness of each section was 8 μm. H&E staining was performed, and the sections were conventionally dewaxed, gradient rehydrated, immersed in hematoxylin solution for 5 minutes, differentiated in differentiation solution for several seconds, and then moved into eosin solution for 5 minutes. Gradient dehydration

Indexed in: [Current Contents/Clinical Medicine] [SCI Expanded] [ISI Alerting System] [ISI Journals Master List] [Index Medicus/MEDLINE] [EMBASE/Excerpta Medica] [Chemical Abstracts/CAS]

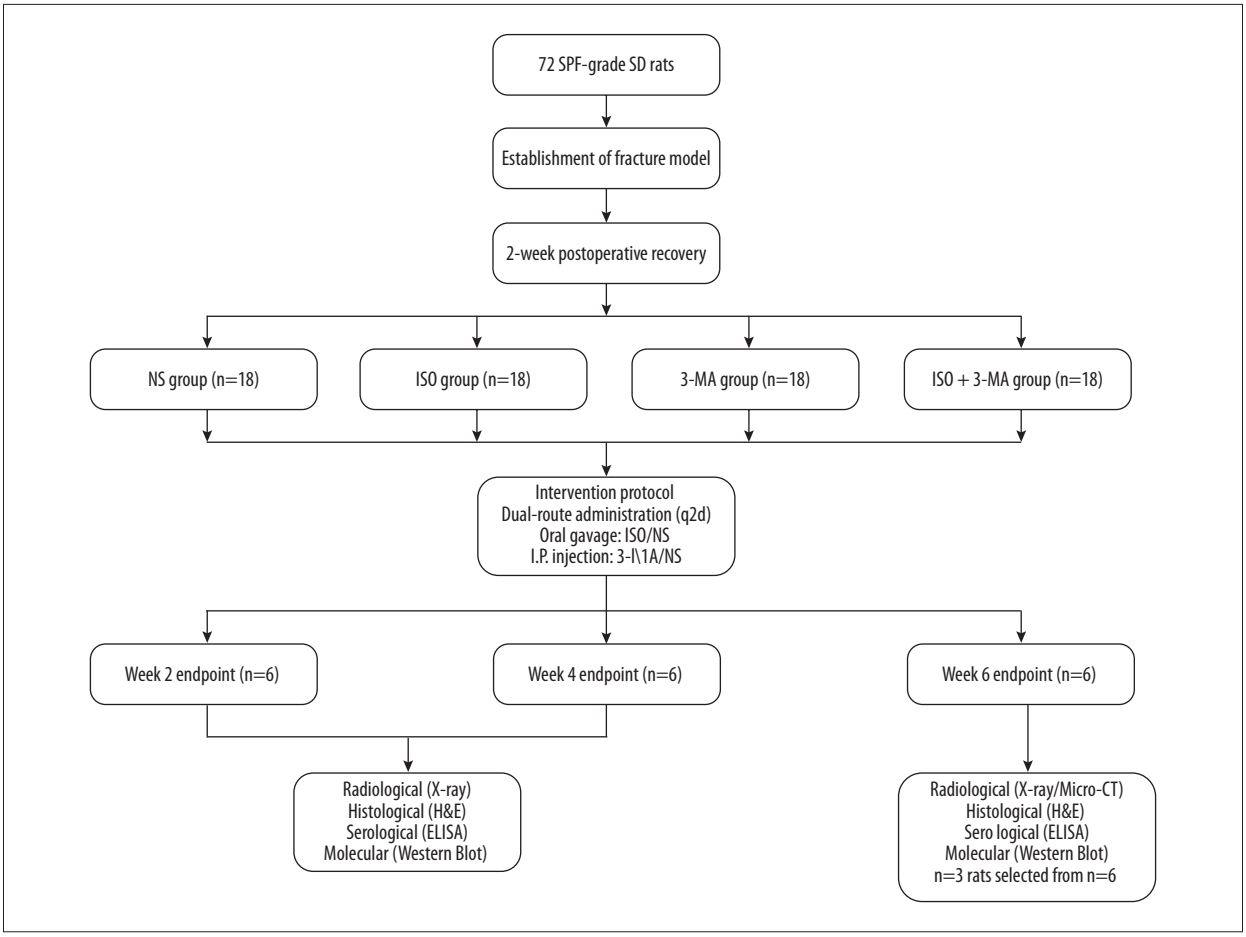

Figure 1. Schematic diagram of the experimental design. A total of 72 specific pathogen-free (SPF) Sprague-Dawley (SD) rats with established mandibular fracture models were randomly assigned to 4 groups (n = 18 per group): normal saline (NS) group, isopsoralen (ISO) group, 3-methyladenine (3-MA) group, and ISO+3-MA group. Each group was further subdivided according to 3 evaluation time points (2, 4, and 6 weeks; n = 6 per time point).

Table 1. Administration plan of rats in each group.

Group	Oral gavage (2 mL, once every 2 days)	Intraperitoneal injection (1 mL, once every 2 days)
NS group	Sterile normal saline	Sterile normal saline
ISO group	ISO 100 mg/kg (in normal saline)	Sterile normal saline
3-MA group	Sterile normal saline	3-MA 30 mg/kg (in normal saline)
ISO+3-MA group	ISO 100 mg/kg (in normal saline)	3-MA 30 mg/kg (in normal saline)

Abbreviations: 3-MA, 3-methyladenine; NS, normal saline; ISO, isopsoralen.

was then performed, and the samples were sealed and placed under a microscope for observation.

Enzyme-Linked Immunosorbent Assay

At 2, 4, and 6 weeks after treatment initiation, blood was taken through the abdominal aorta and centrifuged at 4000 r/min for 16 minutes. The contents of alkaline ALP and OCN were determined according to the instructions of the ELISA kit. The optical density was measured at a wavelength of 450 nm, and the concentration of each sample was calculated.

Indexed in: [Current Contents/Clinical Medicine] [SCI Expanded] [ISI Alerting System] [ISI Journals Master List] [Index Medicus/MEDLINE] [EMBASE/Excerpta Medica] [Chemical Abstracts/CAS]

Table 2. Lane-Sandhu radiographic scoring system.

Item	Description of scoring criteria	Points
Bone formation	No evidence of bone formation	0
	Bone formation occupying 25% of defect	1
	Bone formation occupying 50% of defect	2
	Bone formation occupying 75% of defect	3
	Full gap bone formation	4
Union	Full fracture line	0
	Partial fracture line	2
	Absent fracture line	4
Remodeling	No evidence of remodeling	0
	Remodeling of intramedullary canal	2
	Full remodeling of cortex	4

Western Blotting

At 2, 4, and 6 weeks after administration, the left mandibular bone of each rat was extracted, and the total protein in the mandibular tissue was extracted according to the instructions of the protein extraction kit. Standard curves were prepared with a bicinchoninic acid protein assay kit, and the protein concentration was calculated. The protein was separated via sodium dodecyl sulfate–polyacrylamide gel electrophoresis (120 V, 100 min), transferred to a polyvinylidene fluoride (PVDF) membrane (300 mA, 80 min), and blocked at room temperature for 2 hours with 5% skim milk powder. The PVDF membrane was incubated in Tris-buffered saline with Tween 20 (TBST) and washed 3 times. LC3 (1: 2000), P62 (1: 25,000), and Beclin-1 (1: 5000) primary antibodies were prepared. The PVDF membrane was incubated with the primary antibodies at 4 °C overnight. The membrane was then washed with TBST. Subsequently, the PVDF membrane was incubated with HRP-labeled goat anti-rabbit IgG secondary antibody (1: 5000) and HRP-labeled goat anti-mouse IgG secondary antibody (1: 5000) at room temperature for 1 hour. The developer was added, and bands were visualized using an ultrasensitive multifunctional imager. Protein grayscale values were analyzed using ImageJ software.

Statistical Analysis

All data were analyzed using SPSS 29.0 (IBM Corp, Armonk, NY, USA). Normality was assessed using the Shapiro-Wilk test, and homogeneity of variances was assessed using the Levene test. For each time point (2, 4, and 6 weeks; n = 6 per group), given the independent group design with separate SD rats per group per time point, differences among the 4 groups were evaluated using one-way analysis of variance (ANOVA). When the overall ANOVA was significant ($P < 0.05$), pairwise comparisons between groups were performed using the least significant difference post hoc test. The least significant difference method was selected to maintain statistical power for pre-planned comparisons while controlling the type I error rate under the condition of a significant omnibus test. All data are presented as mean ± standard deviation. $P < 0.05$ was considered statistically significant.

Results

Analysis of Experimental Animals

A total of 80 rats were used in the study. Prior to randomization, 2 rats were excluded as their body weight deviated by more than 20% above the cohort mean. The remaining 78 animals were randomly assigned to experimental groups. During the experimental period, 6 rats were excluded from the final analysis due to predefined criteria: 4 due to accidental death (primarily related to anesthetic complications), and 2 due to severe wound infection. Consequently, data from all 72 rats that completed the experimental protocol without meeting the exclusion criteria were included in the final statistical analysis.

ISO Promoted Bone Graft Growth and Mineralization

As time progressed, fracture sites in all groups gradually healed, with callus formation visible in the bone defect areas. Two weeks postoperatively, the fracture lines remained prominent in the ISO group, while those in the normal saline (NS), ISO, and ISO+3-MA groups showed relative reduction in both the fracture lines and callus volume. By the fourth week, the ISO group exhibited reduced fracture lines and callus, although still clearly visible. The NS, ISO, and ISO+3-MA groups demonstrated indistinct lower margins of fracture ends with callus

Indexed in: [Current Contents/Clinical Medicine] [SCI Expanded] [ISI Alerting System] [ISI Journals Master List] [Index Medicus/MEDLINE] [EMBASE/Excerpta Medica] [Chemical Abstracts/CAS]

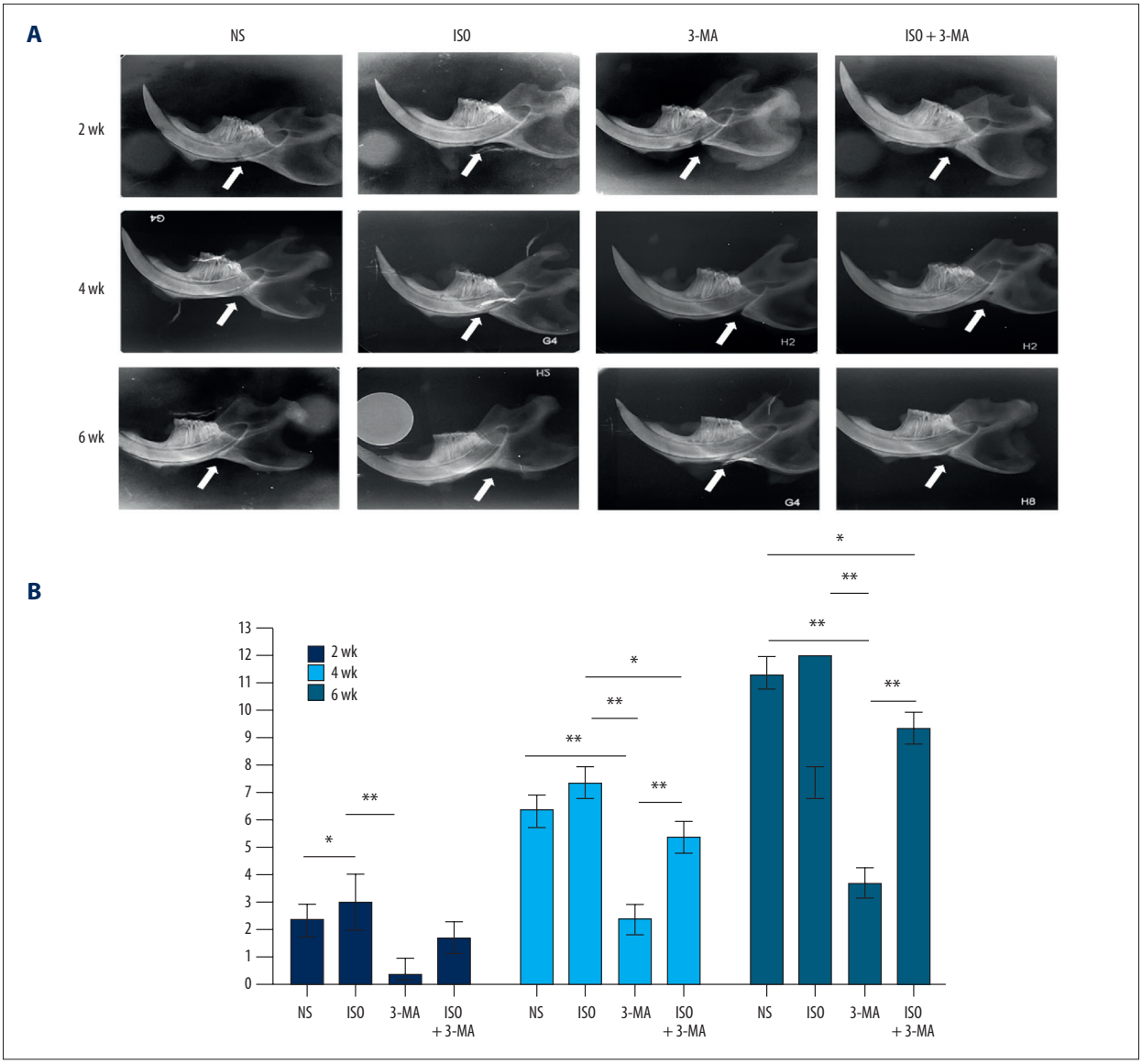

Figure 2. Radiographic findings demonstrating the effects of isopsoralen (ISO) on fracture healing. (**A**) Representative radiographic images of the left mandible at 2, 4, and 6 weeks after administration. White arrows indicate the fracture site. (**B**) Lane-Sandhu radiographic scores in the fracture area (n = 3). Data are presented as mean ± standard deviation. * $P < 0.05$, ** $P < 0.01$ compared with the 3-methyladenine (3-MA) group. Normal saline (NS), ISO, and 3-MA were used as indicated.

formation at the mandibular border. Six weeks postoperatively, the ISO group showed cortical bone formation with reduced fracture lines and callus, although still prominent. The NS, ISO, and ISO+3-MA groups demonstrated good fracture healing with no visible fracture lines (**Figure 2A**). Radiograph evaluations using the Lane-Sandhu scale revealed significantly higher scores in the NS, ISO, and ISO+3-MA groups compared with the 3-MA group ($P < 0.05$), with NS and ISO groups showing markedly higher scores than ISO+3-MA ($P < 0.05$) (**Figure 2B**).

At 6 weeks after administration, the micro-CT results revealed that the callus in the NS group was in the remodeling stage observable from the lateral side, whereas the woven bone in the ISO group was progressively resorbed and replaced by a relatively robust cortical bone structure. Compared with that in the NS group, the cancellous bone density in the 3-MA group was significantly lower. With the addition of ISO, the cancellous bone became denser, the number of trabeculae increased, the trabecular spacing decreased, and the connectivity and extensibility between trabeculae improved (**Figure 3**). The results of the quantitative analysis of the bone parameters in the region of interest are shown in **Table 3**. The bone volume/total volume, bone mineral density, and trabecular number in the NS, ISO, and ISO+3-MA groups were significantly greater than those in the 3-MA group, whereas the

Indexed in: [Current Contents/Clinical Medicine] [SCI Expanded] [ISI Alerting System] [ISI Journals Master List] [Index Medicus/MEDLINE] [EMBASE/Excerpta Medica] [Chemical Abstracts/CAS]

Table 3. Scanning data of bone parameters at 6 weeks after administration in each group.

Group	BV/TV (%)	BMD (mg/cm³)	Tb.N (mm⁻¹)	Tb.Sp (mm)
NS group	1.189 ± 0.056	1.740 ± 0.047	2.060 ± 0.123	0.090 ± 0.012
ISO group	1.273 ± 0.03	1.816 ± 0.015	2.617 ± 0.090[a]	0.082 ± 0.010
3-MA group	0.419 ± 0.088[a,b]	1.051 ± 0.066[a,b]	1.144 ± 0.070[a,b]	0.155 ± 0.007[a,b]
ISO + 3-MAgroup	0.841 ± 0.019[a,b,c]	1.443 ± 0.020[a,b,c]	1.940 ± 0.128[b,c]	0.083 ± 0.009[c]
F	121.2	156.5	88.15	33.06
P	0.0063	0.0058	0.0018	0.0276

Data are presented as mean ± standard deviation; n = 3 per group. [a] Compared with the normal saline (NS) group at the same time point, $P < 0.05$. [b] Compared with the isopsoralen (ISO) group at the same time point, $P < 0.05$. [c] Compared with the 3-methyladenine (3-MA) group at the same time point, $P < 0.05$. Specific *P* values are provided in the corresponding footnotes.
Abbreviations: BV/TV, bone volume/total volume; BMD, bone mineral density; Tb.N, trabecular number; Tb.Sp, trabecular separation.

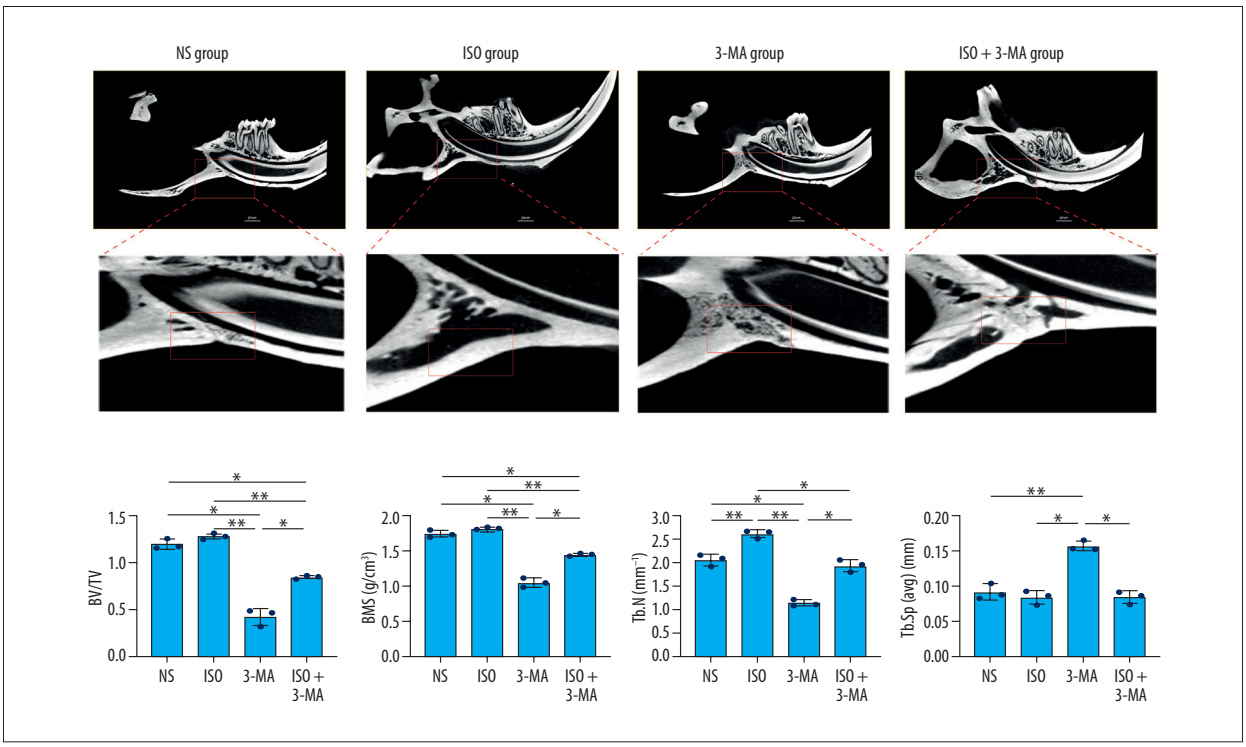

Figure 3. Micro-computed tomography (micro-CT) imaging features of ISO promoting fracture area healing. Comparison of transverse and sagittal micro-CT images and parameters of each group at 6 weeks after administration; The red area indicates the fractured region. Bone volume/total volume (BV/TV), bone mineral density (BMD), and trabecular number in the normal saline (NS), isopsoralen (ISO), and ISO+3-methyladenine (3-MA) groups were significantly greater than those in the 3-MA group, whereas trabecular separation (Tb.Sp) in the 3-MA group was significantly greater than those in the NS, ISO and ISO+3-MA groups (n = 3). Data are presented as mean ± standard deviation (* $P < 0.05$, ** $P < 0.01$).

trabecular separation in the 3-MA group was significantly greater than those in the NS, ISO, and ISO+3-MA groups ($P < 0.05$). Three-dimensional reconstructed images more intuitively demonstrated the bone defect remodeling outcomes across groups. These results indicate that ISO promoted new bone formation in the bone defect area and enhanced bone mass.

Morphological Observation of Callus H&E staining

Figure 4 shows that, over time, the bone reconstruction process in the callus areas of each group gradually advanced. From a histopathological point of view, varying degrees of bone healing were observed in the 4 groups. At 2 weeks after treatment initiation, neovascularization and early trabecular bone structures

Indexed in: [Current Contents/Clinical Medicine] [SCI Expanded] [ISI Alerting System] [ISI Journals Master List] [Index Medicus/MEDLINE] [EMBASE/Excerpta Medica] [Chemical Abstracts/CAS]

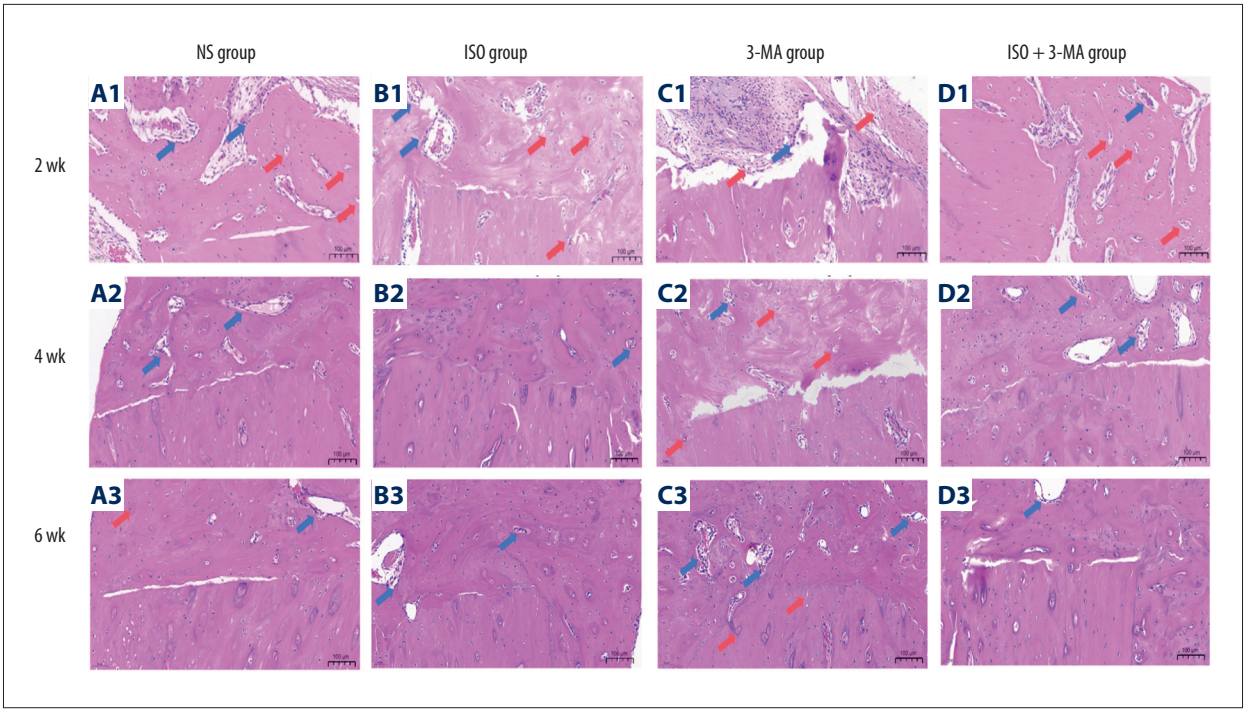

Figure 4. Histological features of the fracture area at 2, 4, and 6 weeks after administration (hematoxylin-eosin staining, ×40 magnification). Panels **A1-A3:** normal saline (NS) group; **B1-B3:** isopsoralen (ISO) group; **C1-C3:** 3-methyladenine (3-MA) group; **D1-D3:** ISO+3-MA group. Columns from top to bottom represent 2, 4, and 6 weeks, respectively. Red arrows indicate neovascularization; blue arrows indicate newly formed trabecular bone and osteoblast accumulation.

were observed in both the NS group and the ISO group, and osteoblasts gathered along the trabecular bone, whereas the trabecular bone density was significantly reduced in the ISO+3-MA group. Only inflammatory cells and fibrous connective tissue were observed in the 3-MA group, and obvious trabecular bone formation was rarely observed (**Figure 4A1-4D1**). At 4 weeks following treatment, the bone trabeculae in the NS and ISO groups thickened, increased in density, were arranged in a braided mesh, and gradually ossified. However, the bone trabeculae density in the ISO+3-MA group was still lower than that in the other 2 groups, while the 3-MA group presented disordered bone trabeculae and low bone trabeculae density (**Figure 4A2-4D2**). At 6 weeks after treatment, the bone trabeculae in the NS group and ISO group were further regularized and tightened, approaching the mature slab bone structure. Although the ISO+3-MA group showed a slab-like arrangement, it was insufficient in density and loose in structure. The 3-MA group exhibited increased trabecular bone quantity compared with the 4-week time point, although the trabecular structure remained as a low-density network with residual fibrous tissue (**Figure 4A3-4D3**).

ISO Improved the Activity and Quantity of ALP and OCN

ALP is a biomarker of early differentiation and bone formation in osteoblasts [16]. **Figure 5 and Tables 4, 5** show that the serum ALP and OCN concentrations changed. At 2 weeks after treatment initiation, the ALP and OCN levels of the NS group, ISO group, and ISO+3-MA group were significantly greater than those of the 3-MA group ($P < 0.05$), and there was no difference among the 3 groups. At the 4-week time point, the ALP levels of the 3 groups were still greater than those of the 3-MA group ($P < 0.05$), the ALP level of the ISO+3-MA group was lower than that of the ISO group ($P < 0.05$), and the OCN level was significantly lower than that of the ISO group and NS group ($P < 0.05$). At 6 weeks after treatment, the ALP levels in the NS and ISO groups remained significantly higher than those in the 3-MA group ($P < 0.05$), with no significant difference between the NS and ISO groups. The ALP level in the ISO+3-MA group was significantly lower than that in the NS group ($P < 0.05$). Similarly, the OCN level in the ISO+3-MA group remained significantly lower than that in both the NS and ISO groups ($P < 0.05$), while the 3-MA group exhibited the lowest OCN levels among all groups at this time point ($P < 0.05$).

ISO Activated Autophagy to Promote Healing of Mandibular Fracture in Rats

Figure 6 and Tables 6-8 demonstrate the temporal changes in autophagy protein expression at fracture sites at 2, 4, and 6 weeks after administration.

Indexed in: [Current Contents/Clinical Medicine] [SCI Expanded] [ISI Alerting System] [ISI Journals Master List] [Index Medicus/MEDLINE] [EMBASE/Excerpta Medica] [Chemical Abstracts/CAS]

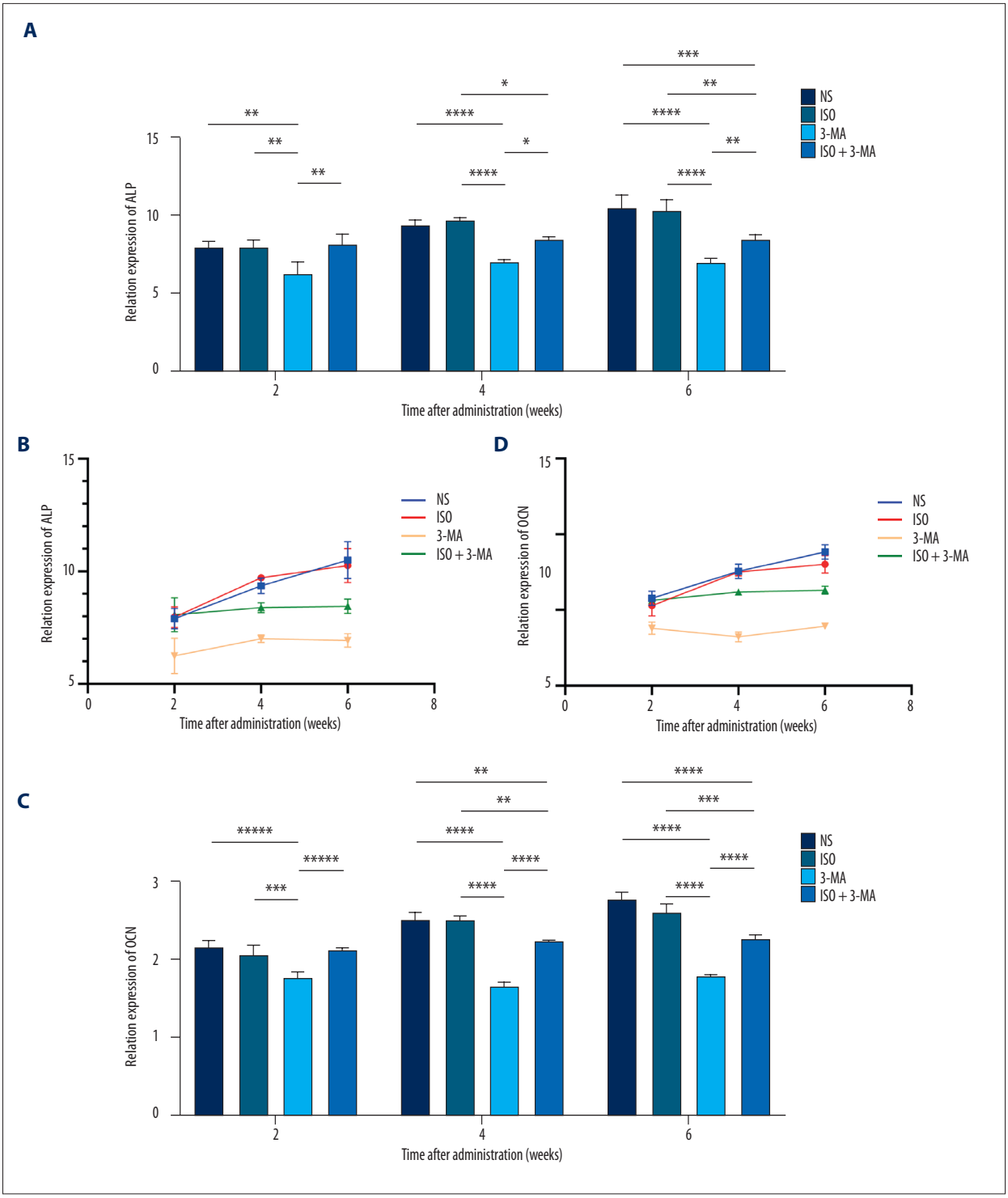

Figure 5. Changes in alkaline phosphatase (ALP) and osteocalcin (OCN) at 2, 4, and 6 weeks after administration. (**A**) Comparison of the serum ALP content between groups at 2, 4 and 6 weeks after dosing. (**B**) Comparison of the changes in the serum ALP content in each group: normal saline (NS) group; isopsoralen (ISO) group; 3-methyladenine (3-MA) group; and ISO+3-MA group. (**C**) Comparison of the serum OCN content at 2, 4, and 6 weeks after administration. (**D**) Comparison of the changes in the serum OCN content in each group (n = 3, * $P < 0.05$, ** $P < 0.01$, *** $P < 0.001$, **** $P < 0.001$).

Indexed in: [Current Contents/Clinical Medicine] [SCI Expanded] [ISI Alerting System] [ISI Journals Master List] [Index Medicus/MEDLINE] [EMBASE/Excerpta Medica] [Chemical Abstracts/CAS]

Table 4. Alkaline phosphatase expression data at each time point in each group.

Group	2 weeks	4 weeks	6 weeks
NS group	7.893 ± 0.45	9.350 ± 0.344	10.493 ± 0.822
ISO group	7.60 ± 0.459	9.713 ± 0.146	10.257 ± 0.749
3-MA group	6.243 ± 0.783[a,b]	7.007 ± 0.171[a,b]	6.27 ± 0.300[a,b]
ISO + 3-MA group	8.070 ± 0.750[c]	8.391 ± 0.218[b,c]	8.443 ± 0.319[a,b,c]
F	7.076	81.46	23.77
P	0.0540	0.0018	0.0066

Data are presented as mean ± standard deviation; n = 3 per group. [a] Compared with the normal saline (NS) group at the same time point, $P < 0.05$. [b] Compared with the isopsoralen (ISO) group at the same time point, $P < 0.05$. [c] Compared with the 3-methyladenine (3-MA) group at the same time point, $P < 0.05$. Specific *P* values are provided in the corresponding footnotes.

Table 5. Osteocalcin expression data at each time point in each group.

Group	2 weeks	4 weeks	6 weeks
NS group	2.153 ± 0.093	2.510 ± 0.095	2.767 ± 0.095
ISO group	2.057 ± 0.137	2.500 ± 0.052	2.603 ± 0.116
3-MA group	1.760 ± 0.082[a,b]	1.643 ± 0.064[a,b]	1.787 ± 0.015[a,b]
ISO + 3-MA group	2.127 ± 0.025[c]	2.237 ± 0.015[a,b,c]	2.260 ± 0.053[a,b,c]
F	12.02	104.2	69.41
P	0.0578	0.0027	0.0124

Data are presented as mean ± standard deviation; n = 3 per group. [a] Compared with the normal saline (NS) group at the same time point, $P < 0.05$. [b] Compared with the isopsoralen (ISO) group at the same time point, $P < 0.05$. [c] Compared with the 3-methyladenine (3-MA) group at the same time point, $P < 0.05$. Specific *P* values are provided in the corresponding footnotes.

P62 Expression

At 2 weeks after administration, the 3-MA group showed the highest P62 levels among all groups ($P < 0.001$), while the ISO group exhibited significantly higher P62 levels than the NS group ($P < 0.05$). At 4 weeks, P62 levels in the ISO group decreased significantly and were lower than those in the NS group ($P < 0.001$), whereas the 3-MA group continued to show elevated P62 ($P < 0.001$). At 6 weeks, P62 levels in the 3-MA group remained significantly higher than those in the NS and ISO groups ($P < 0.05$), while the ISO group showed higher P62 than the NS group ($P < 0.05$). The ISO+3-MA group exhibited significantly lower P62 levels than the 3-MA group at all time points ($P < 0.001$), with levels comparable to those of the NS group at 4 and 6 weeks.

Beclin-1 Expression

At 2 weeks after administration, Beclin-1 expression was significantly lower in both the ISO and 3-MA groups compared with the NS group ($P < 0.001$), with the 3-MA group showing the lowest levels. At 4 weeks, Beclin-1 levels in the ISO group increased significantly and were higher than those in the NS group ($P = 0.0338$), while the 3-MA group remained significantly lower than the NS and ISO groups ($P < 0.001$). At 6 weeks, Beclin-1 levels in the ISO group were comparable to those in the NS group, whereas the 3-MA group continued to show significantly lower levels ($P < 0.001$). The ISO+3-MA group demonstrated significantly higher Beclin-1 expression than the 3-MA group at all time points ($P < 0.01$), with levels comparable to those of the NS group at 4 and 6 weeks.

LC3II/I Ratio

At 2 weeks after administration, the LC3II/I ratio was significantly lower in both the ISO and 3-MA groups compared with the NS group ($P < 0.001$), with the 3-MA group showing the lowest levels. At 4 weeks, this pattern persisted, with both the ISO and 3-MA groups maintaining significantly lower ratios than the NS group ($P < 0.001$). At 6 weeks, although the LC3II/I ratio in the 3-MA group remained significantly lower than that in the NS group ($P < 0.001$), the ratio in the ISO group increased and remained comparable to that of the ISO+3-MA group, with no significant differences between these 2 groups. Notably, the ISO+3-MA group exhibited significantly higher LC3II/I ratios than the 3-MA group at all time points ($P < 0.001$), with levels comparable to those of the ISO group throughout the observation period.

Indexed in: [Current Contents/Clinical Medicine] [SCI Expanded] [ISI Alerting System] [ISI Journals Master List] [Index Medicus/MEDLINE] [EMBASE/Excerpta Medica] [Chemical Abstracts/CAS]

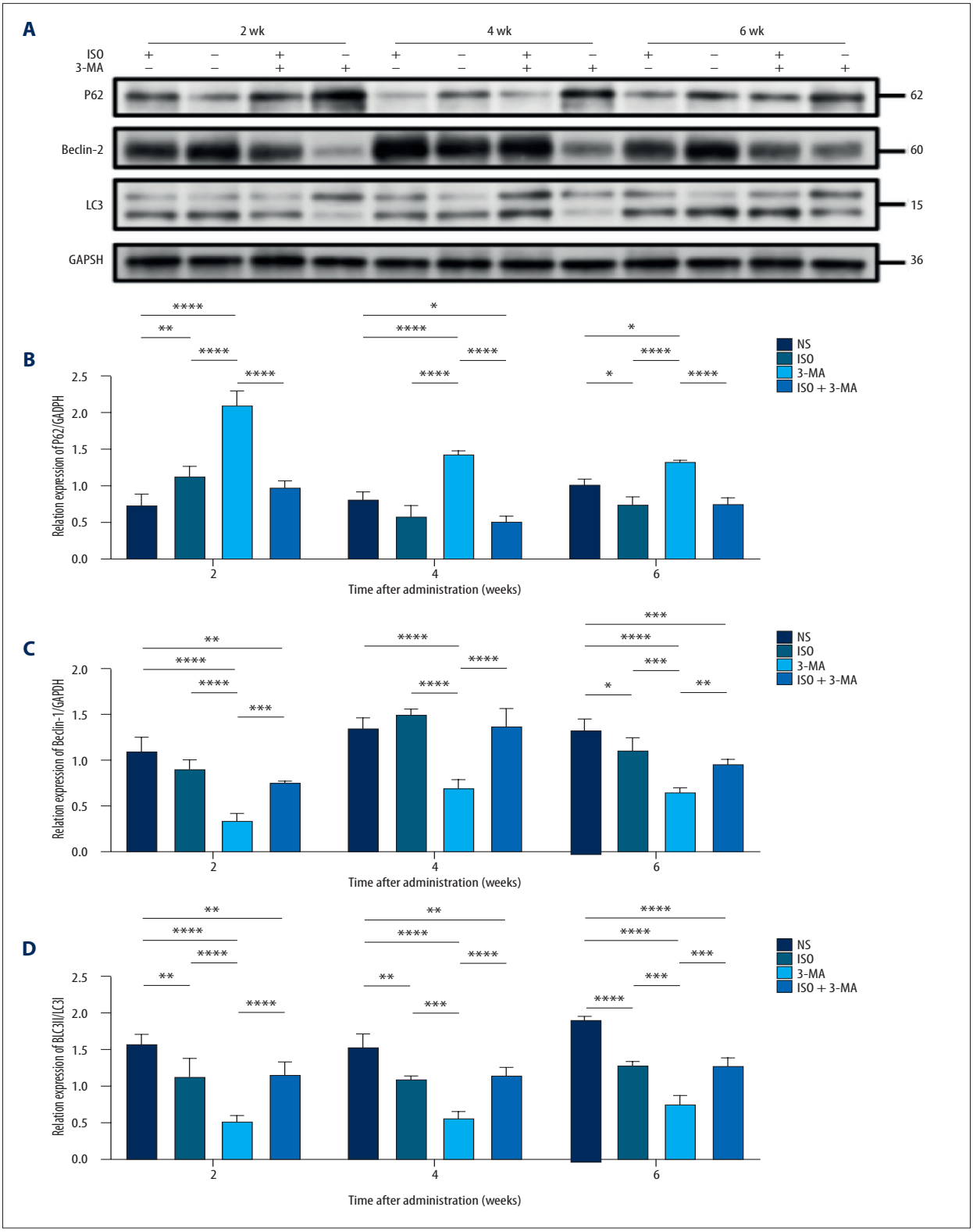

Figure 6. The expression of autophagy-related proteins in the callus region. Expression of autophagy-related proteins in the callus region. (**A**) Representative western blot bands of Beclin-1, LC3, and P62 at 2, 4, and 6 weeks after administration. (**B-D**) Quantitative analysis of P62 (**B**), Beclin-1 (**C**), and LC3II/I ratio (**D**). Data are presented as mean ± standard deviation (n = 3). * $P < 0.05$, ** $P < 0.01$, *** $P < 0.001$, **** $P < 0.0001$.

Indexed in: [Current Contents/Clinical Medicine] [SCI Expanded] [ISI Alerting System] [ISI Journals Master List] [Index Medicus/MEDLINE] [EMBASE/Excerpta Medica] [Chemical Abstracts/CAS]

Table 6. P62 protein expression level (gray value) data at each time point in each group.

Group	2 weeks	4 weeks	6 weeks
NS group	0.724 ± 0.161	0.814 ± 0.103	1.010 ± 0.080
ISO group	1.122 ± 0.147a	0.574 ± 0.153	0.743 ± 0.109[a]
3-MA group	2.092 ± 0.203[a,b]	1.415 ± 0.057[a,b]	1.335 ± 0.007[a,b]
ISO + 3-MA group	0.976 ± 0.09[c]	0.508 ± 0.077[a,c]	0.754 ± 0.074[c]
F	33.35	37.07	32.18
P	0.0128	0.0198	0.0041

Data are presented as mean ± standard deviation; n = 3 per group. [a] Compared with the normal saline (NS) group at the same time point, $P < 0.05$. [b] Compared with the isopsoralen (ISO) group at the same time point, $P < 0.05$. [c] Compared with the 3-methyladenine (3-MA) group at the same time point, $P < 0.05$. Specific *P* values are provided in the corresponding footnotes.

Table 7. Beclin-1 protein expression level (gray value) data at each time point in each group.

Group	2 weeks	4 weeks	6 weeks
NS group	1.093 ± 0.160	1.350 ± 0.111	1.367 ± 0.086
ISO group	0.904 ± 0.095	1.495 ± 0.062	1.103 ± 0.154[a]
3-MA group	0.338 ± 0.081[a,b]	0.689 ± 0.103[a,b]	0.646 ± 0.051[a,b]
ISO + 3-MA group	0.752 ± 0.020[a,c]	1.367 ± 0.200[c]	0.963 ± 0.054[a,c]
F	25.97	18.86	23.24
P	0.0104	0.0227	0.0248

Data are presented as mean ± standard deviation; n = 3 per group. [a] Compared with the normal saline (NS) group at the same time point, $P < 0.05$. [b] Compared with the isopsoralen (ISO) group at the same time point, $P < 0.05$. [c] Compared with the 3-methyladenine (3-MA) group at the same time point, $P < 0.05$. Specific *P* values are provided in the corresponding footnotes.

Table 8. LC3II/I protein expression level (gray value) data at each time point in each group.

Group	2 weeks	4 weeks	6 weeks
NS group	1.568 ± 0.139	1.530 ± 0.185	1.903 ± 0.053
ISO group	1.140 ± 0.245a	1.095 ± 0.044[a]	1.286 ± 0.052[a]
3-MA group	0.522 ± 0.080[a,b]	0.562 ± 0.088[a,b]	0.749 ± 0.137[a,b]
ISO + 3-MA group	1.152 ± 0.180[a,c]	1.148 ± 0.111[a,c]	1.282 ± 0.109[a,c]
F	24.38	26.95	76.66
P	0.0181	0.0192	0.0015

Data are presented as mean ± standard deviation; n = 3 per group. [a] Compared with the normal saline (NS) group at the same time point, $P < 0.05$. [b] Compared with the isopsoralen (ISO) group at the same time point, $P < 0.05$. [c] Compared with the 3-methyladenine (3-MA) group at the same time point, $P < 0.05$. Specific *P* values are provided in the corresponding footnotes.

Discussion

In this study, 3-MA, an autophagy inhibitor, was used to establish a model of autophagy inhibition in mandibular fracture in rats. This model was employed to investigate the effect of ISO intervention, aiming to provide an experimental foundation for precise interventions in mandibular fractures.

ISO Reversed Autophagy Inhibition and Induced Delayed Fracture Healing

Delayed fracture healing or nonunion is often linked to a disruption in local autophagy activity [30]. In this study, 3-MA was used to induce autophagy inhibition and assess the effect of ISO intervention. Imaging revealed a more pronounced fracture line in the 3-MA group than in the other groups across all

Indexed in: [Current Contents/Clinical Medicine] [SCI Expanded] [ISI Alerting System] [ISI Journals Master List] [Index Medicus/MEDLINE] [EMBASE/Excerpta Medica] [Chemical Abstracts/CAS]

time points. The Lane-Sandhu score for fracture healing indicated a significant delay in callus bridging due to autophagy inhibition in the 3-MA group. Conversely, in the ISO group, callus formation occurred earlier, and the closure of the fracture line was accelerated, resulting in a significantly improved Lane-Sandhu score compared with that in the 3-MA group ($P < 0.05$). Histological analysis revealed delayed fracture healing in the 3-MA group, characterized by disorganized trabecular bone, poorly arranged low-density reticular bone, and the presence of fibrous tissue at various time points. Micro-CT analysis of bone parameters further confirmed that ISO could partially reverse the decline in bone mass induced by 3-MA.

Serological analysis revealed that 3-MA notably reduced ALP and OCN levels, whereas ISO significantly elevated them at all time intervals ($P < 0.05$). These findings indicate that ISO may have a limited effect on enhancing healing in individuals with normal autophagy levels but could hold particular therapeutic significance for individuals with compromised autophagic function, such as elderly individuals, individuals with diabetes, and those with postmenopausal osteoporosis.

ISO Regulated Autophagy Level in Callus

Autophagy is involved throughout the entire process of fracture healing, and either excessive or insufficient autophagic activity can compromise the survival and function of osteocytes [23]. Adenosine 5'-monophosphate -activated protein kinase (AMPK), a pivotal enzyme governing cellular energy homeostasis, mediates the initiation and progression of autophagy by inhibiting the phosphorylation of mammalian target of rapamycin (mTOR) and subsequently promoting the phosphorylation of unc-51 like autophagy activating kinase 1 (ULK1) [31]. In addition, existing studies have demonstrated that AMPK activation accelerates fracture healing by enhancing autophagy, thereby improving the differentiation and mineralization of osteoblasts [32]. Moreover, activation of the Wnt/β-catenin pathway has been shown to alleviate hydrogen peroxide–induced injury in osteoblasts [33]. Furthermore, psoralen-mediated osteogenic differentiation of periodontal ligament stem cells is regulated with the involvement of the mTOR pathway [34].

The present study involved the dynamic monitoring of 3 autophagy marker proteins, namely, Beclin-1, LC3II/I, and P62, to elucidate the temporal regulatory effects of ISO on autophagy within the jaw callus. Beclin-1 is a crucial protein in the initiation of autophagy. Elevated levels of Beclin-1 indicate the activation of autophagy [35,36]. In the NS group, there was a consistent increase in autophagy initiation, indicating sustained activity throughout the jaw healing process. Autophagy was significantly suppressed by 3-MA. However, in the ISO+3-MA group, the expression returned to baseline levels after 4 weeks, suggesting that ISO has the ability to reverse the inhibition of autophagy initiation. LC3II binds to the autophagy membrane and plays a role in autophagy initiation and maturation following autophagy induction. The conversion of LC3I to LC3II occurs during autophagy, and a higher LC3II/I ratio typically indicates increased autophagic activity [37]. In the present study, the LC3II/I ratio continuously increased between 2 and 6 weeks, indicating increased autophagy and maturation during the intermediate and late stages of the healing process. The ratio significantly decreased in the 3-MA group, whereas treatment with ISO only partially restored it, suggesting that ISO had a limited effect on autophagy. P62 is a substrate for autophagy, and its expression inversely correlates with degradation efficiency [38]. Following ISO treatment, P62 levels briefly increased at 2 weeks, indicating potential inhibition of lysosomal degradation in the initial phase. P62 levels subsequently significantly decreased at 4 weeks, which coincided with the restoration of lysosomal function. Furthermore, at 6 weeks, P62 levels decreased again, whereas Beclin-1 and LC3II/I were concurrently downregulated, suggesting that prolonged intervention could trigger alternative ubiquitin-proteasome degradation pathways to maintain protein homeostasis.

In conclusion, the regulation of autophagy in jaw calluses by ISO follows a precise temporal pattern: autophagy flow is primarily suppressed in the initial stage (2 weeks), subsequently reinstated through improved lysosomal function in the intermediate stage (4 weeks), and eventually declines in the later stage (6 weeks). During this decline, P62 is degraded through alternative pathways to maintain the protein homeostasis necessary for callus remodeling. This temporal regulation exhibits a bidirectional and sequential pattern, aligning with the reported bidirectional autophagy regulatory traits of ISO in various other models.

Research Limitations and Prospects

The present study demonstrates that ISO effectively ameliorates delayed mandibular fracture healing induced by autophagy inhibition, whereas its pro-healing effects are limited under conditions of normal autophagy. These findings suggest that the clinical translational value of ISO may be primarily confined to patient populations with impaired autophagic function, underscoring the importance of patient stratification based on autophagic status in future clinical applications.

Despite these promising findings, several limitations should be acknowledged. First, the sample size in the present mandibular fracture model was relatively small, and key parameters—including the optimal dosage, route of administration, and evaluation endpoints—remain to be further optimized. Second, although 3-MA is widely used as a pharmacological

Indexed in: [Current Contents/Clinical Medicine] [SCI Expanded] [ISI Alerting System] [ISI Journals Master List] [Index Medicus/MEDLINE] [EMBASE/Excerpta Medica] [Chemical Abstracts/CAS]

autophagy inhibitor, its potential off-target effects, including inhibition of class III PI3K and interference with other cellular processes, warrant caution in interpreting the causal role of autophagy in ISO-mediated bone healing. Future studies employing genetic approaches—such as siRNA-mediated knockdown of autophagy-related genes (eg, Atg5, Atg7, or Beclin1) in osteoblast or osteoclast precursor cells—are necessary to establish the specific contribution of autophagy to the pro-healing effects of ISO.

In addition to efficacy considerations, the safety profile of ISO is a critical factor for its clinical translation. Although no overt signs of toxicity (eg, abnormal body weight loss or reduced food intake) were observed in SD rats following intraperitoneal administration of 100 mg/kg ISO every other day for 2 to 6 weeks, accumulating preclinical and clinical evidence indicates that ISO and its parent plant *Psoralea corylifolia* L. may exhibit potential organ toxicity under specific conditions, predominantly affecting the liver and reproductive system. Toxicological studies have demonstrated that ISO can alter organ coefficients in rats, including decreased cardiac and increased ovarian coefficients in females, as well as elevated testicular, cardiac, and adrenal coefficients in males, suggesting potential effects on the reproductive system in both sexes. Metabolomic analyses further reveal that ISO treatment may disrupt amino acid metabolism, potentially contributing to metabolic disturbances [39].

Hepatotoxicity remains a key concern in the safety evaluation of ISO. Short-term exposure to high-dose ISO (80 mg/kg) has been shown to disrupt bile acid homeostasis by inhibiting efflux transporters and amino acid–conjugating enzymes, leading to liver injury [40]. Clinical case reports have also implicated formulations containing psoralen and ISO in drug-induced liver injury [41]. Mechanistic studies suggest that ISO and psoralen may impair bile acid metabolism by downregulating key transporters such as CYP7A1, CYP27A1, BSEP, and OSTα, resulting in intrahepatic accumulation of unconjugated bile acids—an effect that appears more pronounced in males [42]. Notably, overexpression of SULT1E1 has been shown to alleviate such cholestatic liver injury, providing potential clues for protective strategies [43].

The safety profile of ISO exhibits dose-dependent complexity. Pharmacokinetic data indicate high bioavailability of ISO in beagle dogs, suggesting that careful optimization of dosing regimens is necessary to avoid cumulative toxicity [44]. Supporting this notion, continuous administration of 20 mg/kg ISO for 35 days in a male C57BL/6 mouse model of osteoarthritis effectively alleviated symptoms without detectable hepatorenal toxicity [45]. In the present study, the intermittent dosing schedule (every other day) and intraperitoneal route of administration may have contributed to the favorable safety profile by minimizing sustained drug accumulation and circumventing first-pass metabolism, thereby reducing direct toxic stimulation to hepatocytes.

Methodological limitations should also be considered. Although randomization was performed using a random number table, strict allocation concealment and blinding of outcome assessors (eg, for radiographic scoring and histological analysis) were not implemented, which may have introduced assessment bias. Future studies should incorporate independent blinded assessors to validate the current findings.

Collectively, while ISO exhibits promising therapeutic potential in fracture healing, its clinical translation must be predicated on comprehensive risk assessment. Future translational investigations should integrate multidimensional toxicological evaluations—including assessments of hepatic and renal function, histopathological examination, reproductive organ analysis, and metabolomic profiling—and further explore sex differences in ISO metabolism and toxicity. The development of precision therapeutic regimens based on minimally effective doses and optimized routes of administration will be critical to balancing the efficacy and safety of ISO. Moreover, multicenter, large-sample translational studies focusing on sequential therapeutic strategies combining ISO with autophagy agonists or other osteogenic agents may facilitate the development of novel, individualized treatment approaches for mandibular fractures.

Conclusions

This study focused on the regulatory effect of ISO on mandibular fracture healing and identified the autophagy-mediated mechanism for the first time, filling the gap in research on ISO and autophagy in maxillofacial fracture healing. The autophagy inhibitor 3-MA was used to establish a mandibular fracture model with impaired healing, and the temporal regulatory effect of ISO on autophagy in jaw calluses was clarified. These findings provide a theoretical basis and experimental support for precise clinical intervention in patients with autophagy-deficient fractures.

Institution Where Work Was Done

School of Stomatology, Zunyi Medical University, , Zunyi, Guizhou, PR China.

Declaration of Figures' Authenticity

All figures submitted have been created by the authors who confirm that the images are original with no duplication and have not been previously published in whole or in part.

Indexed in: [Current Contents/Clinical Medicine] [SCI Expanded] [ISI Alerting System] [ISI Journals Master List] [Index Medicus/MEDLINE] [EMBASE/Excerpta Medica] [Chemical Abstracts/CAS]

References:

1. Wu C, Yan J, Ge C, et al. Macrophage membrane-reversibly camouflaged nanotherapeutics accelerate fracture healing by fostering MSCs recruitment and osteogenic differentiation. J Nanobiotechnology. 2024;22(1):411
2. Chen H, Jia Z, He X, et al. Burden and trends of facial fractures in China and the United States based on GBD 2021 analysis. Sci Rep. 2025;15(1):8328
3. Şahar D, Gerçek AO, Bayrakçi N. Risk factors of mandibular angle fractures based on digital reduction method: A retrospective analysis. BMC Oral Health. 2025;25(1):1338
4. Aulakh KK, Gumber TK, Sandhu S. Prognosis of teeth in the line of jaw fractures. Dent Traumatol. 2017;33(2):126-32
5. Stanford-Moore G, Murr AH. Mandibular angle fractures. Facial Plast Surg Clin North Am. 2022;30(1):109-16
6. Breulmann FL, Hatt LP, Schmitz B, et al. Prognostic and therapeutic potential of microRNAs for fracture healing processes and non-union fractures: A systematic review. Clin Transl Med. 2023;13(1):e1161
7. Wu X, Shen T, Ji W, et al. lncRNA CASC11 regulates the progress of delayed fracture healing via sponging miR-150-3p. J Orthop Surg Res. 2024;19(1):757
8. Wildemann B, Ignatius A, Leung F, et al. Non-union bone fractures. Nat Rev Dis Primers. 2021;7(1):57
9. Qiu ZC, Tang XY, Wu QC, et al. A new strategy for discovering effective substances and mechanisms of traditional Chinese medicine based on standardized drug containing plasma and the absorbed ingredients composition, a case study of Xian-Ling-Gu-Bao capsules. J Ethnopharmacol. 2021;279:114396
10. Yang J, Wen L, Jiang Y, Yang B. Natural estrogen receptor modulators and their heterologous biosynthesis. Trends Endocrinol Metab. 2019;30(1):66-76
11. Chen L, Chen S, Sun P, et al. *Psoralea corylifolia* L.: A comprehensive review of its botany, traditional uses, phytochemistry, pharmacology, toxicology, quality control and pharmacokinetics. Chin Med. 2023;18(1):4
12. Meng D, Dong Y, Shang Q, Sun Z. Anti-tumor effect and hepatotoxicity mechanisms of psoralen. Front Pharmacol. 2024;15:1442700
13. Shi Z, Gao J, Pan J, et al. A systematic review on the safety of *Psoraleae fructus*: Potential risks, toxic characteristics, underlying mechanisms and detoxification methods. Chin J Nat Med. 2022;20(11):805-13
14. Feng Y, Chen Y, Wu X, et al. Interplay of energy metabolism and autophagy. Autophagy. 2024;20(1):4-14
15. Song J, Zhang H, Cao X, et al. Pbs2 regulates late-stage macroautophagy in *Saccharomyces cerevisiae*. Animal Model Exp Med. 2025;8(7):1321-27
16. Yin X, Zhou C, Li J, et al. Correction to: Autophagy in bone homeostasis and the onset of osteoporosis. Bone Res. 2020;8:36 [Erratum for: Bone Res. 2019;7:28]
17. Wang J, Zhang Y, Cao J, et al. The role of autophagy in bone metabolism and clinical significance. Autophagy. 2023;19(9):2409-27
18. Zhu C, Shen S, Zhang S, et al. Autophagy in bone remodeling: a regulator of oxidative stress. Front Endocrinol (Lausanne). 2022;13:898634
19. Li X, Xu J, Dai B, et al. Targeting autophagy in osteoporosis: From pathophysiology to potential therapy. Ageing Res Rev. 2020;62:101098
20. Pareek G, Kundu M. Physiological functions of ULK1/2. J Mol Biol. 2024;436(15):168472
21. Fan S, Yue L, Wan W, et al. Inhibition of autophagy by a small molecule through covalent modification of the LC3 protein. Angew Chem Int Ed Engl. 2021;60(50):26105-14
22. Wu Y, Liu H, Wang Q, et al. Neoeriocitrin targeting Beclin1 deubiquitination and autophagy in osteogenic differentiation of human dental pulp stem cells. Adv Sci (Weinh). 2025;12(43):e04378
23. James A, Hendrixson JA, Kadhim I, et al. Elevation of master autophagy regulator Tfeb in osteoblast lineage cells increases bone mass and strength. JCI Insight. 2025;10(17):e191688
24. Cheng NT, Meng H, Ma LF, et al. Role of autophagy in the progression of osteoarthritis: The autophagy inhibitor, 3-methyladenine, aggravates the severity of experimental osteoarthritis. Int J Mol Med. 2017;39(5):1224-32
25. Ma C, Zhang X, Mo X, et al. Xie-Bai-San increases NSCLC cells sensitivity to gefitinib by inhibiting Beclin-1 mediated autophagosome formation. Phytomedicine. 2024;125:155351
26. Zeng X, Zhang YD, Ma RY, et al. Activated Drp1 regulates p62-mediated autophagic flux and aggravates inflammation in cerebral ischemia-reperfusion via the ROS-RIP1/RIP3-exosome axis. Mil Med Res. 2022;9(1):25
27. Ge YS, Huang CM, Shen J, et al. PD0325901 alleviates thrombin-inhibited osteogenic differentiation through an IL-1β-activated feedback loop between MEK-Erk1/2 and NF-κB signal pathways: Insights from bioinformatics and experimental verification. Front Immunol. 2026;17:1730337
28. Choi YY, Jin SC, Song M, et al. *Cervus elaphus sibiricus* (deer antler) extract alleviates osteoporosis via dual modulation of osteoblast and osteoclast activity in ovariectomy-induced mice on network pharmacology. J Ethnopharmacol. 2026;355(Pt A):120669
29. Li S, Li Y, Jiang Z, et al. Efficacy of total flavonoids of *Rhizoma drynariae* on the blood vessels and the bone graft in the induced membrane. Phytomedicine. 2022;99:153995
30. Lao Z, Liu Z, Ji W, et al. Irisolidone enhances osteoblast differentiation via the AMPK-ULK1-autophagy Axis to accelerate osteoporotic fracture repair. Biochem Pharmacol. 2025 Aug 13;242(Pt 1):117234
31. Meng W, Luo L, Xiao Z, et al. Liver kinase B1 maintains natural killer cell survival by regulating redox homeostasis. Cell Death Dis. 2026;17(1):413
32. Li H, Li D, Ma Z, et al. Defective autophagy in osteoblasts induces endoplasmic reticulum stress and causes remarkable bone loss. Autophagy. 2018;14(10):1726-41
33. Li YP, Wu B, Liang J, Li F. Isopsoralen ameliorates H_2O_2-induced damage in osteoblasts via activating the Wnt/β-catenin pathway. Exp Ther Med. 2019;18(3):1899-906
34. Wang Y, Zhang H, Yu J, et al. Psoralen-mediated regulation of osteogenic differentiation of periodontal ligament stem cells: Involvement of the mTOR pathway. Front Cell Dev Biol. 2025;13:1634945
35. Hu S, Lv L, Hu W, Shen J. Quercetin improves myocardial ischemia-reperfusion injury by regulating macrophage M2 polarization through Bcl-2/Beclin-1 complex. Eur J Med Res. 2025;30(1):780
36. Cao Z, Tian K, Ran Y, et al. Beclin-1: A therapeutic target at the intersection of autophagy, immunotherapy, and cancer treatment. Front Immunol. 2024;15:1506426
37. Coelho PP, Park M. LEAP: A novel LC3C-dependent pathway connects autophagy, endocytic trafficking and signaling. Autophagy. 2023;19(4):1354-56
38. Qian H, Ding WX. SQSTM1/p62 and hepatic Mallory-Denk body formation in alcohol-associated liver disease. Am J Pathol. 2023;193(10):1415-26
39. Zhang Y, Yuan XM, Wang YF, et al. Isopsoralen induces different subchronic toxicities and metabolomic outcomes between male and female Wistar rats. Regul Toxicol Pharmacol. 2019;103:1-9
40. Men WJ, Meng ZJ, Wang Q, et al. The changes of hepatic bile acid synthesis and transport and bile acids profiles in isopsoralen-induced liver injury C57BL/6J mice. Pharm Biol. 2022;60(1):1701-9
41. Yang A, Chen J, Ma Y, et al. Studies on the metabolites difference of psoralen/isopsoralen in human and six mammalian liver microsomes in vitro by UHPLC-MS/MS. J Pharm Biomed Anal. 2017;141:200-9
42. Chen MY, Wang Q, Meng ZJ, et al. Psoralen induces liver injury and affects hepatic bile acids metabolism in female and male C57BL/6J mice. Phytother Res. 2023;37(6):2280-89
43. Wu Y, Xu Y, Cai H, et al. Overexpression of SULT1E1 alleviates salt-processed *Psoraleae fructus*-induced cholestatic liver damage. Chin Herb Med. 2024;17(2):392-403
44. Li SP, Atikanmu WF, Rahima AL. [Pharmacokinetics of three pairs isomers of Caraway in Beagle dogs based on UPLC-MS/MS.] Zhongguo Zhong Yao Za Zhi. 2025;50(24):7013-21 [in Chinese]
45. Zhang A, Li S, Qiao J, et al. Isopsoralen alleviates osteoarthritis by modulating the MAPK/NF-κB signaling pathway and regulating the structure of gut microbiota. J Ethnopharmacol. 2026;361:121257

Indexed in: [Current Contents/Clinical Medicine] [SCI Expanded] [ISI Alerting System] [ISI Journals Master List] [Index Medicus/MEDLINE] [EMBASE/Excerpta Medica] [Chemical Abstracts/CAS]